APPENDIX F
PREVIOUS GEOPHYSICAL CHARACTERIZATION AND MONITORING AT THE ORFRC

Geophysical methods, including radar, seismic, and complex electrical crosshole data and surface electrical and seismic data have been used on a limited basis for both characterization and monitoring at the ORFRC. Here, we briefly describe the use of some of those data, illustrating the strengths of using different geophysical techniques and acquisition geometries to meet different objectives.

Hydrogeological and Geochemical Characterization

Both surface and crosshole tomographic geophysical data have been used in the saprolite and carbonate gravel (Areas 3 and 2, respectively) to delineate large scale geologic structure, nitrate plume boundaries, and local-scale fracture zonation. Surface electrical and seismic data were originally used in a reconnaissance mode to choose the location for the Plot 2 biostimulation experiment. Figure F1 illustrates electrical resistivity variations along the A-A' transect adjacent to the S-3 Ponds area. Comparison with measured nitrate concentrations (obtained from wellbore locations) shows that at this site, zones of low electrical resistivity (or high electrical conductivity) are correlated with zones having higher nitrate concentration. This observation is consistent with our other studies at the site, which suggest that electrical methods are more sensitive to variations in pore fluid ionic strength at the FRC than to hydrogeological heterogeneity. Superimposed on the electrical profile are contour lines indicating the seismic velocity gradients obtained from surface seismic data. These velocity contours can be interpreted in terms of gross lithological structure. The results of this surface geophysical study, which is further described by Watson et al. (2005), were used to define the Plot 2 biostimulation study site location, highlighted by the black rectangle in Figure F1.
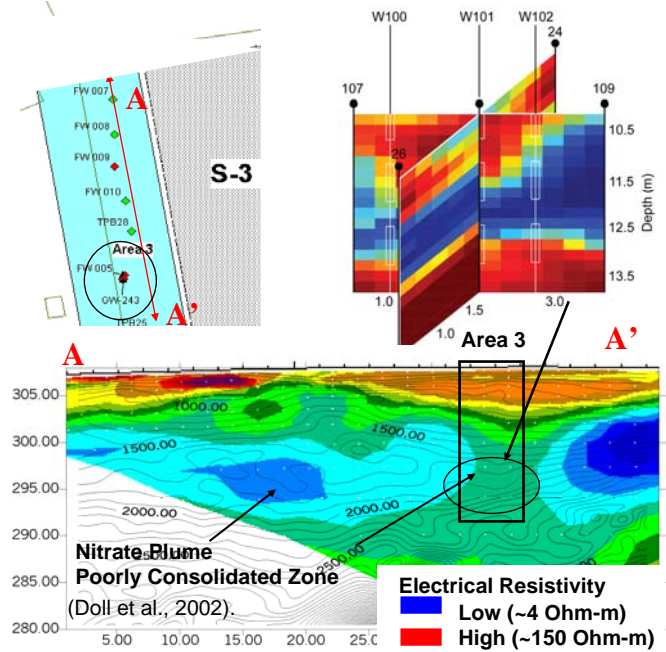

Figure F1 Top left: locations of surface and tomographic geophysical data acquisition. Top right: probability of being in the high hydraulic conductivity fracture zone obtained using seismic tomographic data in the experimental area, where blue indicates the highest probability (Chen et al., 2006); Bottom – surface electrical resistivity and seismic velocity data, indicating large scale plume and lithological zonation (Watson et al.,2005) .

Successful bioremediation requires co-occurrence of the bacteria, electron acceptor, electron donor, and the contaminant (e.g., Scheibe et al., 2006). As local-scale heterogeneity surrounding the injection well can influence the distribution of many (if not all) of these components, high-resolution characterization can be extremely helpful for both guiding and evaluating developing remedial treatments. For this purpose, we colleted crosshole seismic data in conjunction with the biostimulation experiment conducted at Plot 2 study site. As seismic velocity is sensitive to the 'stiffness' of a material, we hypothesized that fracture zones would be less stiff than the surrounding competent rock and would thus have a lower seismic velocity. Through development of a joint hydrological-geophysical estimation procedure, we used the seismic tomographic data to estimate the probability of observing the high permeability fracture zone within the Plot 2 study site (Figure F1). These estimates revealed that the target biostimulation zone

has a varying thickness and dip, and is sometimes laterally discontinuous. Indeed, comparison of tracer and uranium biostimulation experimental results at the study site with the fracture estimation suggests that the seismic method was useful for delineating zones that were hydraulically isolated from the amendment injection area. Details about the high-resolution fracture characterization advances are given in Chen et al. (2006). The information gained from the combined geophysical and more standard characterization methods could also be useful for understanding and predicting the impact of heterogeneity when scaling up remediation efforts from small test plots to a full scale remediation effort.
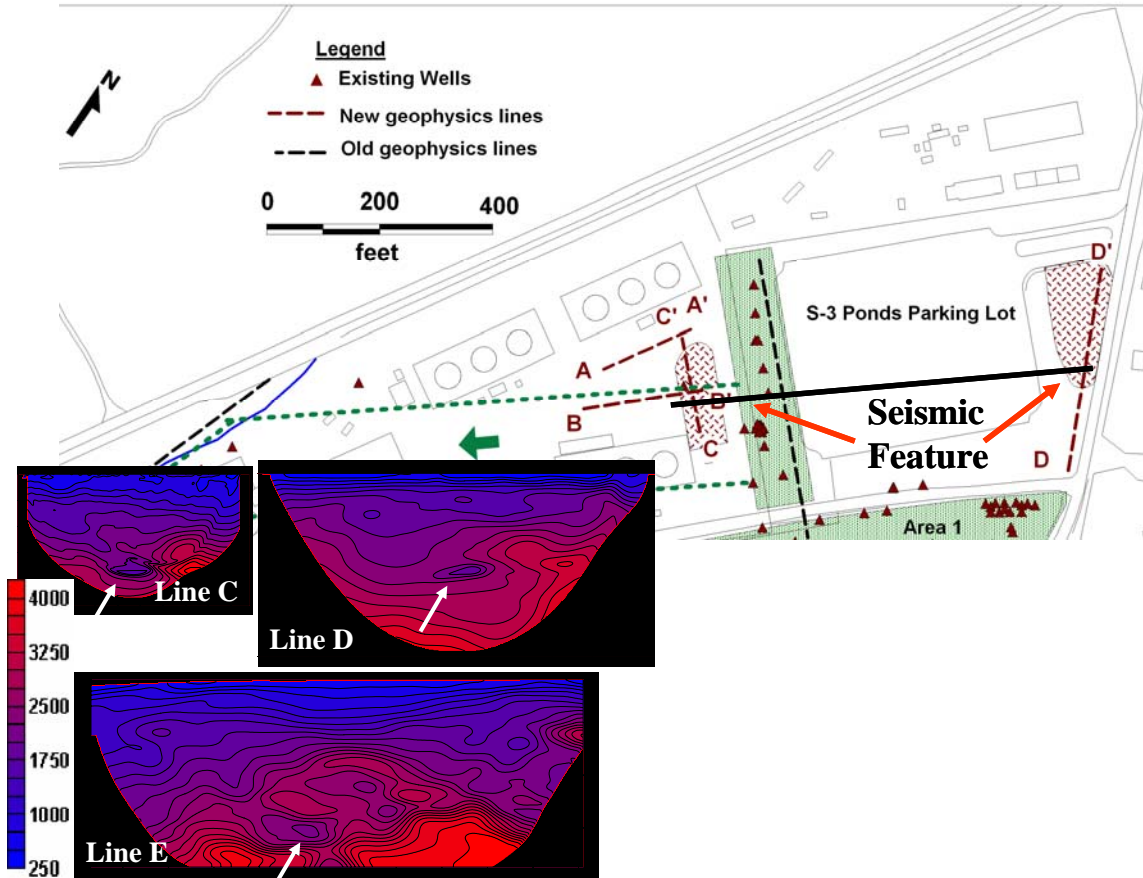

Figure F2 Map of seismic survey lines and seismic tomography results that reveal a common low-velocity feature along strike at ~30m depth.

Surface seismic tomography data was collected from 3 parallel seismic lines located near the S-3 Ponds and aligned perpendicular to strike and the direction of groundwater flow. A low seismic velocity feature was identified in each of the lines at a depth of about 30 m (Fig. F2). The low velocity feature appears to be oriented along bedding planes and the direction of groundwater flow. We have not drilled into the seismic feature to determine what is causing this geophysical response but this may be important to do since the feature may be impacting contaminant migration at the site.
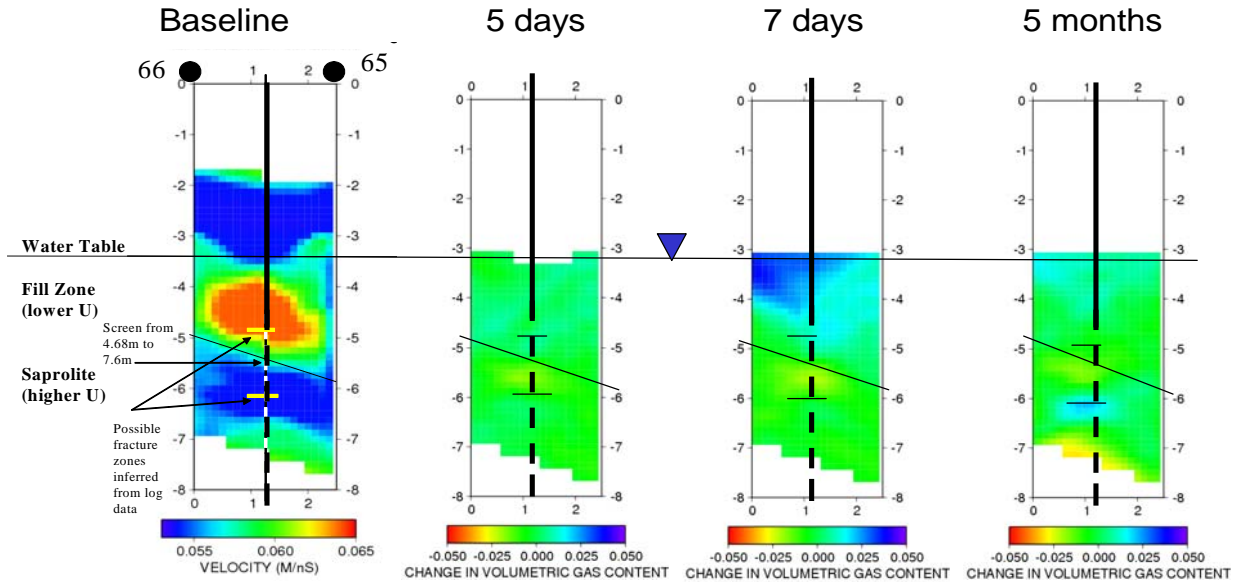
Figure F3 Left panel: hydrogeological zonation interpreted through comparison of baseline radar and seismic tomographic data with wellbore electrical, temperature, and acoustic televiewer logs. Right three figures: estimate of gas evolved at different times after injection of ethanol into the center well.

Process Monitoring

Time-lapse tomographic data have also been collected at the FRC site to elucidate processes that occur during biostimulation. These studies have included the use of SP data to indicate changes in redox conditions during biostimulation at Plot 3, and use of crosshole electrical and radar methods to estimate gas and precipitate evolution at Areas 1 and 2, respectively. Because of the presence of high nitrate groundwater at the FRC and the need to reduce nitrate prior to Uranium reduction, biostimulation experiments at the FRC are expected to produce significant N_2 or N_2O gas. In collaboration with Dr. Jack Istok, we used time-lapse radar tomographic velocity data and a mixing model to provide estimates of gas evolution associated with a push-pull test conducted in the center well shown in Figure F2. This figure illustrates that the generated gas quickly migrated into the overlying fill and was temporally trapped beneath the water table. This study illustrates the value of geophysical data for monitoring remediation processes and again highlights the impact of local-scale heterogeneity on remedial treatments.

Azimuthal Resistivity Surveys: During a bromide tracer test conducted in Plot 3, the field plot was monitored using time-lapse azimuthal electrical resistivity surveys. A plan diagram of well locations, well hits for the bromide tracer, and position of the resistivity electrodes is provided in Figure F4.
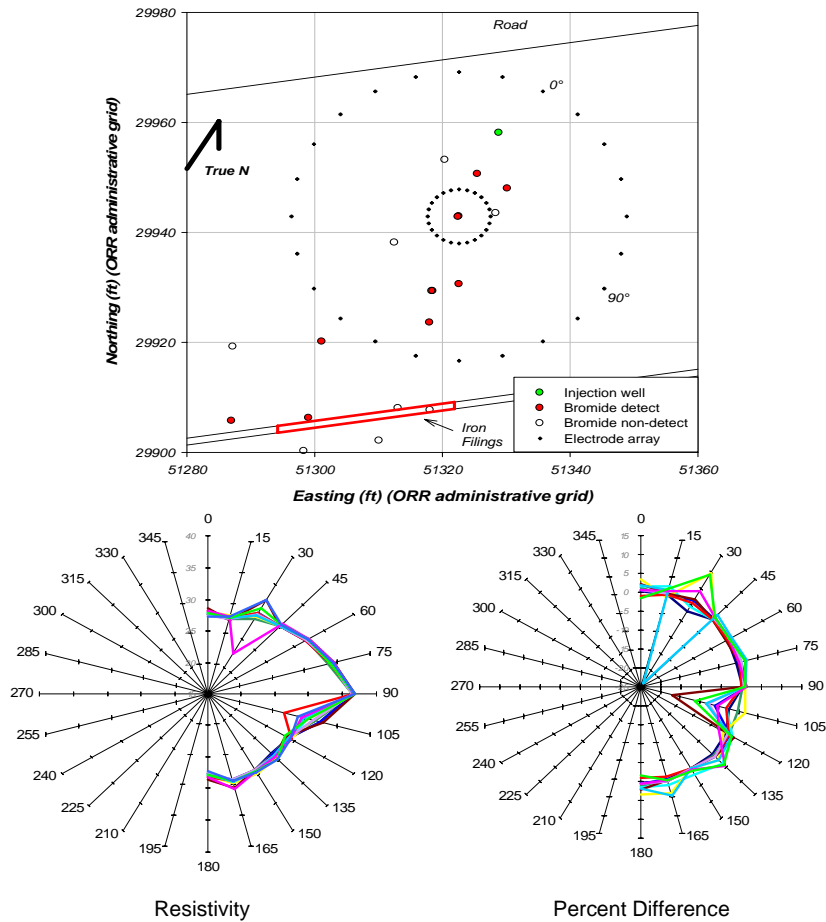
F-3

Figure F4 Upper panel: Map of the well field for bromide tracer test in the carbonate gravel indicating injection and monitoring wells and the azimuthal resistivity electrode arrays. Lower left panel: Snapshot of the time-lapse azimuthal electrical resistivity data collected during hour 45 of the tracer test. The multiple curves represent data collected at earlier times. Note the significant deviations at 30° and 105° (relative to true north); these orientations align with the principal tracer flow direction (30°) and regional strike (105°). Lower right panel: data from the lower left panel presented as percent change from initial (preinjection) conditions.

The main resistivity changes took place only in the 30° and the 105° directions (Fig. F4). The 30° direction is about 50° from the inferred NNW to SSE flow direction as estimated from monitoring wells. The 105° direction is roughly parallel to regional strike. Although we cannot completely rule out the possibility that the resistivity fluctuations were caused by site specific stray currents, there are two lines of evidence that point to their being real. First, most of the averaged resistivities remained stable throughout the experiment, fluctuating only a few percent about background. Second, some of the large resistivity changes remained stable for hours, from one set of measurements to the next. For instance, from hour 36 to hour 45, a significant decrease in resistivity in the 105° direction stayed stable, and from hour 45 to hour 48 the measurement at 30° remained stable. This stability would be unlikely if stray currents were the source of the fluctuations. We believe this test shows that azimuthal resistivity measurements have application to time-varying processes, and also that significant site noise from low frequency stray currents can be overcome by resistivity averaging and thus permit useful time-lapse data to be collected.

Time-lapse imaging of tracer test with Electromagnetic Induction: A dilute KCl solution was injected in well FW024 of Plot 2 displacing the highly conductive nitrate- rich contaminated fluids. Imaging of flushing and tracer migration was conducted by logging 10 wells repetitively over a 1-week period with an EM-39 borehole conductivity logger. The data was used to produce 3-D images (Fig. F5) of the tracer migration in the subsurface over time. These data and images can be used to map preferred migration pathways and the extent of treatment zones.
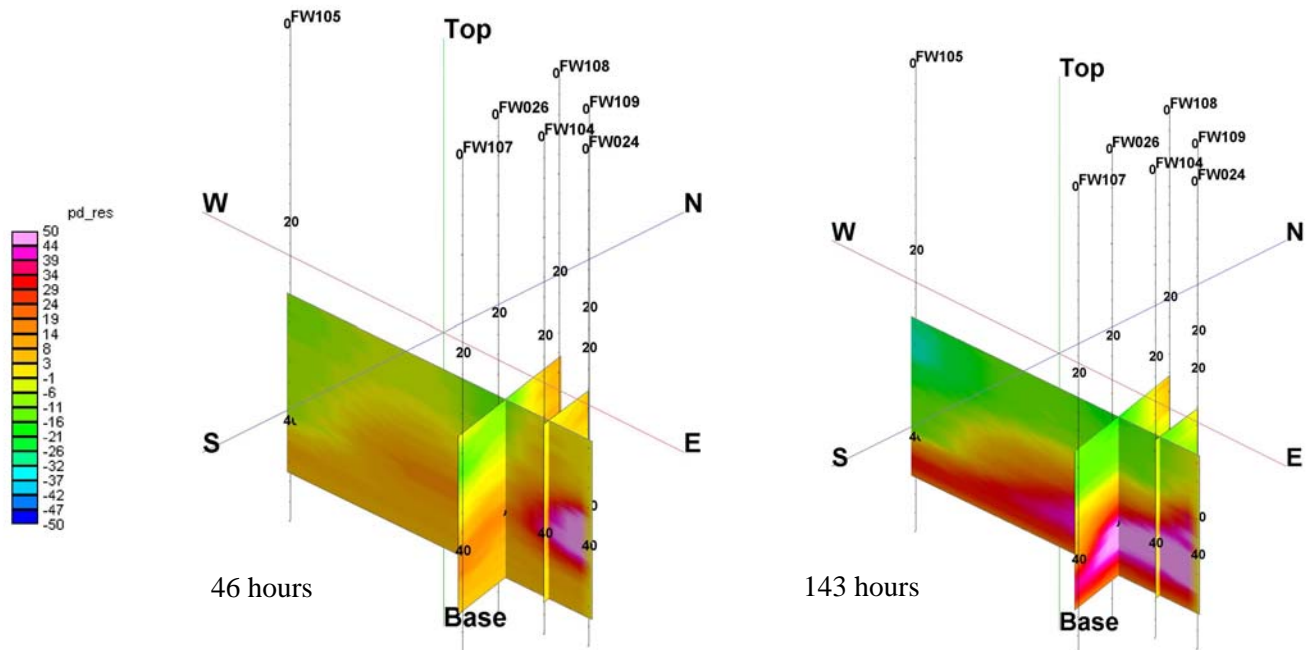

Figure F5 Time-lapse imaging of low conductivity tracer solution injected at Plot 2 using electromagnetic induction techniques showing percent difference in conductivity from the start of the tracer injection. Red and pink indicates location of tracer solution in subsurface.

References

Chen, J., S. Hubbard, J. Peterson, K. Williams, M. Fienen, P. Jardine, D. Watson. Development of a joint hydrogeophysical inversion approach and application to a contaminated fractured aquifer. 2006. Water Resources Research, 42:W06425, doi:10.1029/2005WR004694

Scheibe, T. D., Y. Fang, C. J. Murray, E. E. Roden, J. Chen, Y.-J. Chien, S. C. Brooks, and S. S. Hubbard. 2006. Transport and biogeochemical reaction of metals in a physically and chemically heterogeneous aquifer. Geosphere 2(4):220-235. doi: 10.1130/GES00029.1

Watson, D. B., W. E. Doll, T. J. Gamey, J. R. Sheehan, and P. M. Jardine. 2005. Plume and lithologic profiling with surface resistivity and seismic tomography. Ground Water 43(2):169–177.